Shap. Mem. Superelasticity (2019) 5:136–146
https://doi.org/10.1007/s40830-018-00203-4

Assessment of Entropy Differences from Critical Stress Versus Temperature Martensitic Transformation Data in Cu-Based Shape-Memory Alloys

J. L. Pelegrina[1,2,3] · A. M. Condó[1,2,3] · A. Fernández Guillermet[1,2,3]

Published online: 9 December 2018

Abstract The entropy differences per unit volume (ΔS^{trans}) between the close-packed phases in a martensitic transformation (MT) in Cu-based shape-memory alloys are obtained from mechanical tests by measuring, as a function of temperature (T), the critical resolved stress (τ). Specifically, ΔS^{trans} values are obtained from the slope of τ versus T plots by invoking a relation which is straightforwardly derived from the classical Clausius–Clapeyron equation, viz., $\frac{d\tau}{dT} = -\frac{\Delta S^{trans}}{\gamma}$, where γ is the transformation shear strain. Motivated by the significant scatter of the so obtained ΔS^{trans} values, the thermodynamic bases of such evaluation procedure have been revised, by accounting for the nucleation step of a martensite plate. The interface, elastic strain, and chemical contributions to the Gibbs energy of nucleation have been considered. A new expression of the type $\frac{d\tau}{dT} = \mathbf{\Omega} - \frac{\Delta S^{trans}}{\gamma}$ is obtained, where the $\mathbf{\Omega}$ term involves the elastic properties and their temperature dependence. The new $\tau - T - \Delta S^{trans}$ relation is used to assess the ΔS^{trans} values corresponding to the 2H/18R and 18R/6R MTs in Cu–Al–Ni and Cu–Zn–Al alloys. The ΔS^{trans} values obtained by the present approach fall on a scatter band centered around the zero value.

Keywords Stress-induced martensitic transformation · Entropy of transformation · CuZnAl · CuNiAl

✉ J. L. Pelegrina
jlp201@cab.cnea.gov.ar

A. M. Condó
adriana@cab.cnea.gov.ar

A. Fernández Guillermet
a.f.guillermet@gmail.com

[1] Centro Atómico Bariloche, CNEA, Av. E. Bustillo 9500 R8402AGP Bariloche, Argentina

[2] Instituto Balseiro, CNEA and Universidad Nacional de Cuyo, Bariloche, Argentina

[3] CONICET, Bariloche, Argentina

Introduction

Thermodynamic Background

In the experimental determination of thermodynamic quantities, it is generally agreed that the martensitic transformations (MTs) allow a high precision in the determination of the relative phase stability between austenite and martensite, due to the small temperature and/or stress hysteresis between direct transformation and reverse transformation. The thermodynamic values obtained by common calorimetry, tension, and/or compression experiments agree well within the typical uncertainties. This is, in particular, the case of the single crystals in NiTi [1] and in Cu-based alloys [2]. In particular, for Cu-based alloys, there has been a considerable interest in the estimation of the entropy difference (ΔS) by analyzing the results of mechanical tests where the critical resolved stress (τ) at which the MT is induced is determined as a function of temperature (T). Then, from the slope of the experimental τ versus T plots, an entropy difference is evaluated using a form of the classical Clapeyron equation usually referred to, in the present research field, as the Clausius–Clapeyron (CC) equation, viz.,

$$\frac{d\tau}{dT} = -\frac{\Delta S}{V\gamma} = -\frac{\Delta S^{trans}}{\gamma}, \quad (1)$$

where ΔS^{trans} is the entropy difference between structures per unit volume, and γ is the transformation shear strain. Concerning the type of behavior expected, it should be remarked that, for Cu-based shape-memory alloys, the stress and temperature dependencies of ΔS^{trans} and of γ are small [3]. As a consequence, an almost constant slope is predicted by Eq. (1) for those systems, which has often been referred to as "the CC behavior."

As a motivation of the present study in the following section, it is shown that Eq. (1) has been used in several alloy systems in the last decades.

Applications of Eq. (1) to Study the "the CC behavior"

Already in 1976 Otsuka et al. [4] stress-induced the MT to two different martensitic structures in a Cu–Al–Ni alloy. Although they find different slopes in the linear behavior between critical stress and temperature, the calculated enthalpies agreed within experimental scatter.

In 1984, Miyazaki and Otsuka [5] used Eq. (1) to calculate the heat of transformation in a $Ti_{50}Ni_{47}Fe_3$ alloy for the transformation to the R-phase and to martensite. They reported some discrepancies with the calorimetric measurements and associated them to a wrong determination of the strain associated to the transitions.

Miyazaki and Otsuka [6] studied in 1986 NiTi alloys above and below the equiatomic composition. They reported higher slopes for the transformation to the R-phase as compared to that to martensite, which was ascribed to the smallness in the transition strain due to the R-phase transition.

In 1988, Stachowiak and McCormick [7] performed calorimetric measurements under constant load in a Ti–50.2 at.% Ni alloy. They detected the starting temperatures for the transformation to the R-phase, to martensite and the reverse transition to austenite, as a function of the applied stress. Having found the linearity between stress and temperature, they compared the experimentally determined slopes with the ones calculated from Eq. (1) using the measured transformation enthalpies and equilibrium temperatures.

Pelegrina and Ahlers in 1992 [8] used mechanical experiments to determine ΔS^{trans} in Cu–Zn–Al alloys. They concluded that there exists a composition dependence for the entropy of transformation between austenite and martensite.

In 1998, Orgéas and Favier [9] performed mechanical testing experiments on equiatomic NiTi under three different deformation modes: tension, compression, and simple shear. The comparison of the measured stress–temperature slopes to the data from the literature allowed them to conclude that their results are strongly influenced by the initial treatment conditions.

Šittner et al. [10] performed in 1999 tension/compression tests in Cu–Al–Zn–Mn polycrystals and compared the experimental results with the predictions of a simple model. The use of the CC equation was found to be of crucial importance for the model, since the temperature and orientation dependence of the transformation stresses were introduced through it.

In 2004, Brinson et al. [11] stress induced the MT in polycrystalline NiTi. They determined the latent heat effect by measuring simultaneously the temperature decay and stress decay. Since both magnitudes approach equilibrium values at identical times, they concluded that the temperature decay after latent heat release is primarily responsible for the stress relaxation observed. After this transient time, the CC behavior could be measured and compared with other published values.

Otsuka and Ren [12] in 2005 used Eq. (1) to differentiate the case of stress-induced transformation from slip, with the latter having a negative temperature dependence of the critical stress.

In 2007, Auguet et al. [13] analyzed the use of shape-memory alloys for damping applications in family houses. They identified the more relevant macroscopic thermomechanical properties characterizing the process of transforming mechanical energy into heat, mentioning the CC equation as a fundamental relation.

Kockar et al. [14] measured in 2008 the stress–temperature slopes in ultrafine-grained NiTi fabricated using equal-channel angular extrusion (ECAE). Using Eq. (1) they evaluated the transformation entropy and deduced the changes in the elastic strain and irreversible energies, comparing hot-rolled samples with the ECAE-processed ones.

In 2011, Olbricht et al. [15] studied the transitions in ultrafine-grained Ni-rich NiTi. They constructed CC-type of plots by combining mechanical tests, electrical resistance measurements under constant load, and calorimetric determinations. The small discrepancies between the experimental techniques were related to features of each transition.

In the following section, the results of applying Eq. (1) to particular cases in Cu-based alloys are reviewed.

The Problem of the Entropy Differences in Cu-Based Alloys

A qualitative summary of the relative phase stability in Cu-based shape-memory alloys is presented in Fig. 1. All the martensitic phases are close-packed structures, whose stability depends on composition, temperature, and applied stress. The three phases of most interest are denoted as 3R,

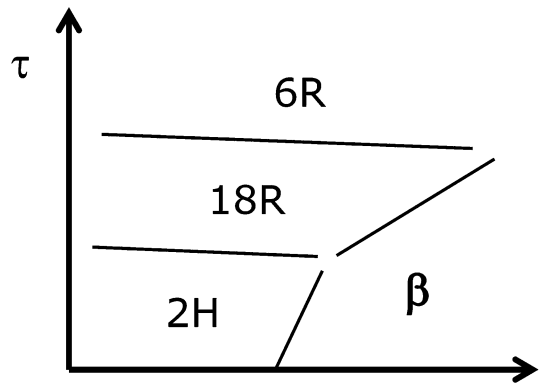

Fig. 1 Schematic phase diagram showing the relations between the various phase fields of the martensitic phases typically found in Cu-based alloys

9R, and 2H for inherited B2 order, with ABC, ABCB-CACAB, and AB stacking sequences, respectively. If instead of B2, the DO_3 or $L2_1$ order is present, the first two structures duplicate the number of planes in the sequence, and are accordingly renamed as 6R and 18R, respectively [16].

In addition to the usual austenite-to-martensite transformation induced either by temperature or by the application of stresses (e.g., β to 18R), Fig. 1 suggests that there exists the possibility of a transition between the martensites (e.g., 2H to 18R) only induced by stresses. Examples of the such transformations can be found for Cu–Al–Ni [17–21], Cu–Zn–Al [22–27], Cu–Al–Be [28, 29], Cu–Sn [30], and Cu–Zn [22, 31].

In the experimental τ versus T phase diagram of these alloys, the phase field limit between 2H and 18R and/or that between 18R and 6R, are roughly linear, and in most of the cases show a small negative slope (see Table 1). A comparison of the reported $d\tau/dT$ values is shown in Fig. 2 for those cases which will be treated in the present study. It should be emphasized that only the experimental data obtained from transitions involving single variant phases were selected, in order to diminish the risk of nucleation occurring in additional sites. The measurements plotted in Fig. 2 should therefore be considered as the most compatible with the bases of the thermodynamic model to be developed in "Thermodynamic Modeling" section.

In view of the significant scatter in the $d\tau/dT$ values in Fig. 2, some authors have assumed that the probable slope is zero [26]. Alternatively, others attempted to estimate an entropy difference between the martensitic phases using Eq. (1) [19, 27, 29]. In the latter cases, the resulting ΔS^{trans} values are small in magnitude and positive, but the value $\Delta S^{trans} = 0$ is claimed to fall outside the experimental scatter. Such discrepancy between assuming $\Delta S^{trans} = 0$ or > 0 has originated a long-standing controversy with two important implications for the understanding of the transformations in Cu-based shape-memory alloys. First, thermodynamically, a first-order transition with $\Delta S^{trans} = 0$ could not be induced by a change in temperature. This is not the common situation for the MTs, where quantities such as M_S and T_0 are used to discuss stability. As a second consequence, a negligible value of the entropy difference between martensitic phases has been related with an entropy difference between austenite and martensite ($\Delta S^{mart/aust}$) varying linearly only with the electron concentration [32]. Alternatively, the nonnegligible ΔS^{trans} led to a model for $\Delta S^{mart/aust}$ dependent on the structure of the martensite but not on composition [33]. This controversy is still unresolved and motivates the following attempt to shed some light on the discrepancies between the reported ΔS^{trans} values for the systems referred to in Fig. 2.

Scope of the Present Work

Specifically, in the present study, the evaluation of ΔS^{trans} from τ versus T data will be reanalyzed by considering an early remark by Olson and Cohen [34] about the importance of an accurate account of the strain contribution in evaluating thermodynamic properties from both calorimetric and mechanical testing experiments. Such method of analysis has been recently applied by Laplanche et al. [35] to the reorientation of martensitic variants in NiTi alloys. Those authors analyzed the negative slope of the stress–temperature curve in terms of a model based on classical nucleation theory, and accounting for the variation of the elastic constants with temperature.

Inspired by these two [34, 35] enlightening contributions, in the following discussion and for Cu-based shape-memory alloys, the possibility will be explored of (i) deducing a more accurate relation between the experimental slope $d\tau/dT$ of MT data and the entropy difference ΔS^{trans}; (ii) using such relation to determine the most probable ΔS^{trans} values; and (iii) shedding some light on the $\Delta S^{mart/aust}$ controversy.

Thermodynamic Modeling

The MT occurs as a nucleation and growth process. The latter is normally visualized as a macroscopic shear. Notwithstanding, the very beginning of the nucleation event is normally treated within the oblate-spheroidal-embryo approach [36].

The pioneering study by Kaufmann and Cohen [36–38] started a long tradition of thermodynamic studies of the MT. The key conceptual strategy [39] is to express the Gibbs energy change (ΔG) involved in the nucleation of a martensitic embryo as the sum of interface ("inter"),

Table 1 Experimental information on the applied stress σ versus temperature T slopes for Cu-based shape-memory alloys, reported by various authors

Systems	References	Phases	$d\sigma/dT$ (MPa/K)	Tensile axis	M_S (K)	s
Cu–Al–Ni	[17]	18R → 2H	− 0.053	[2 11 16]	248	0.206
	[18]	2H → 18R	− 0.416	[1 3 20]	306	0.466
		18R → 2H	+ 0.014			
		18R → 6R	− 0.496			0.469
		6R → 18R	+ 0.173			
	[19]	2H ↔ 18R	− 0.206	[1 3 20]	308	0.466
		18R ↔ 6R	− 0.139			0.469
		18R → 6R	− 0.174			
	[20]	18R → 6R	− 0.290	∼[0 0 1]	268	0.496
		6R → 18R	+ 0.100			
	[21]	18R → 6R	− 0.295	∼[0 0 1]	276	0.496
		18R → 6R	− 0.240	∼[0 0 1]	281	0.496
		18R → 6R	− 0.302	∼[0 0 1]	243	0.496
Cu–Zn–Al	[22]	18R → 6R	0.175	∼[0 2 15]	272	0.477
	[23]	18R → 6R	− 0.627	∼[2 5 43]	254	0.478
		18R → 6R	− 0.165	∼[1 4 43]	248	0.484
		18R → 6R	− 0.244	∼[2 4 57]	253	0.487
		18R → 6R	− 0.203	∼[3 5 35]	223	0.467
		18R → 6R	− 0.231	∼[1 5 44]	242	0.480
	[24]	18R → 6R	− 0.459	[5 8 13]	263	0.208
	[25]	18R → 6R	0.00	[2 5 57]	246	0.484
	[26]	2H ↔ 18R	+ 0.35	[6 10 43]	270	0.429
		2H ↔ 18R	− 0.31	[2 5 57]	246	0.481
		2H ↔ 18R	− 0.56	[1 1 3]	223	0.357
		2H ↔ 18R	− 0.34	[6 7 37]	200	0.441
		2H ↔ 18R	− 0.64	[3 3 11]	184	0.393
		2H ↔ 18R	(− 1.92)	[1 5 6]	263	0.130
		2H ↔ 18R	− 0.38	[6 20 63]	237	0.400
		2H ↔ 18R	− 0.41	[0 0 1]	214	0.493
		2H ↔ 18R	+ 0.53	[5 6 54]	178	0.470
		2H ↔ 18R	− 0.86	[11 26 64]	235	0.349
		2H ↔ 18R	(+ 3.80)	[5 6 16]	256	0.342
		2H ↔ 18R	+ 0.85	[3 4 34]	229	0.469
		2H ↔ 18R	− 0.42	[3 8 64]	195	0.472
	[27]	2H → 18R	− 0.336	[3 5 22]	276	0.432
		18R → 2H	− 0.011			
Cu–Al–Be	[28]	18R → 6R	− 0.3	∼[0 0 1]	263	0.496
	[29]	18R → 6R	− 0.286	[0 1 8]	296	0.479
		6R → 18R	− 0.190			
Cu–Sn	[30]	18R → 2H	− 0.326	[1 5 30]	180	0.463
		18R → 6R	− 0.180			0.465
Cu–Zn	[22]	18R → 6R	− 0.027	∼[3 5 8]	141	0.204
	[31]	18R → 6R	− 0.51	not available	153	not available
		18R → 6R	− 0.28	not available	153	not available

The values labeled 2H ↔ 18R and 18R ↔ 6R were determined as the average of the direct and reverse transformations, and the values labeled 2H → 18R, 18R → 2H, 18R → 6R , and 6R → 18R correspond to single transformations. The tensile axis, the austenite-to-martensite transformation temperature at zero stress (M_S) and the Schmid factor s, involved in the relation $\tau = s\sigma$, are given for each sample. The slope values in parentheses are considered unrealistic and thus excluded from the present analysis

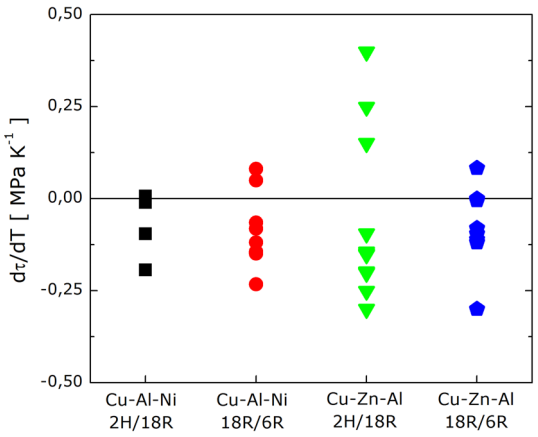

Fig. 2 Experimental values for the slopes in the critical resolved shear stress versus temperature plots in Cu–Al–Ni and Cu–Zn–Al alloys. The specific transition between martensitic phases is indicated at the bottom. The data stem from the measurements presented in Table 1

elastic strain ("elast"), and chemical (or phase transformation, "trans") contributions:

$$\Delta G = \Delta G^{\text{inter}} + \Delta G^{\text{elast}} + \Delta G^{\text{trans}}. \tag{2}$$

Among these contributions, ΔG^{inter} is proportional to the area (A) of the embryo, whereas ΔG^{elast} and ΔG^{trans} are proportional to its volume (V). By introducing quantities expressing the interface contribution per unit area (Γ^{inter}) and the elastic strain (Δg^{elast}) and transformation (Δg^{trans}) contributions per unit volume, Eq. (2) is usually [40] written as follows:

$$\Delta G = A\Gamma^{\text{inter}} + V\Delta g^{\text{elast}} + V\Delta g^{\text{trans}}. \tag{3}$$

The Elastic Strain Contribution

The elastic strain contribution to ΔG in Eq. (3) for the formation of a martensitic oblate-spheroidal embryo of radius r and semithickness c is given by [41]

$$\Delta g^{\text{elast}} = K^{\text{elast}} \frac{c}{r}, \tag{4}$$

where K^{elast} is

$$K^{\text{elast}} = \frac{\pi\mu(2-\nu)}{8(1-\nu)}\gamma^2 + \frac{\pi\mu}{4(1-\nu)}\xi^2. \tag{5}$$

In Eq. (5), ν and μ (G for some authors) are the Poisson ratio and the shear modulus, respectively, for the matrix. For the MT, the quantities γ and ξ represent the shear in the habit plane and the normal deformation, respectively. As the MT in Cu-based alloys, to be treated in "Assessment of ΔS^{trans} for Cu-Based Shape-Memory Alloys" section, implies no volume change, $\xi = 0$ will be assumed [3, 35] and thus γ represents the transformation shear strain.

Gibbs Energy of Formation

For the nucleation of a thin oblate-spheroidal embryo [36] with $V = \frac{4}{3}\pi r^2 c$ and $A \approx 2\pi r^2$, Eq. (3) becomes

$$\Delta G = 2\pi r^2 \Gamma^{\text{inter}} + \frac{1}{6}\pi^2 r c^2 \frac{\mu(2-\nu)}{(1-\nu)}\gamma^2 + \frac{4}{3}\pi r^2 c \Delta g^{\text{trans}}. \tag{6}$$

Even though the above equation considers the nucleation in an elastically isotropic material, it has been successfully used to describe the martensite reorientation process in the anisotropic NiTi system [35]. Encouraged by these [35] results, the present study will explore the applicability of Eq. (6) to assess entropy differences for the MT in Cu-based shape-memory alloys ("Assessment of ΔS^{trans} for Cu-Based Shape-Memory Alloys" section). To this aim, the following thermodynamic picture was developed.

Consider a martensite nucleus of a fixed size coexisting in metastable equilibrium with the matrix at the start of the MT. It will remain in such condition if the differential changes in the quantities Γ^{inter}, μ, ν and Δg^{trans} do not modify its Gibbs energy of formation. Mathematically this corresponds to the condition $\mathrm{d}(\Delta G) = 0$, which leads to the following differential equation:

$$\begin{aligned} &2\pi r^2 \mathrm{d}\left(\Gamma^{\text{inter}}\right) + \frac{1}{6}\pi^2 r c^2 \frac{(2-\nu)}{(1-\nu)}\gamma^2 \mathrm{d}\mu \\ &+ \frac{1}{6}\pi^2 r c^2 \frac{\mu}{(1-\nu)^2}\gamma^2 \mathrm{d}\nu + \frac{4}{3}\pi r^2 c \mathrm{d}(\Delta g^{\text{trans}}) \\ &= 0, \end{aligned} \tag{7}$$

where $\mathrm{d}(\Gamma^{\text{inter}})$, $\mathrm{d}\mu$, $\mathrm{d}\nu$, and $\mathrm{d}(\Delta g^{\text{trans}})$ will be treated in the next section.

Independent Variables and General Relations

The problem of establishing the dependencies of the physical parameters upon the relevant variables of the model is a frequent one. As an example, it is worth mentioning the case in [42], where an attempt to account for the effect of sample size upon the various parameters within a thermodynamic framework was hampered by the lack of experimental information. A similar problem will be dealt with in the following.

The differentials $\mathrm{d}(\Gamma^{\text{inter}})$, $\mathrm{d}\mu$, $\mathrm{d}\nu$, and $\mathrm{d}(\Delta g^{\text{trans}})$ will be expressed in terms of the independent variables temperature (T) and force (f) as follows:

$$\mathrm{d}\left(\Gamma^{\text{inter}}\right) = \frac{\partial(\Gamma^{\text{inter}})}{\partial T}\mathrm{d}T + \frac{\partial(\Gamma^{\text{inter}})}{\partial f}\mathrm{d}f, \tag{8}$$

$$\mathrm{d}\mu = \frac{\mathrm{d}\mu}{\mathrm{d}T}\mathrm{d}T, \tag{9}$$

$$\mathrm{d}v = \frac{\mathrm{d}v}{\mathrm{d}T}\mathrm{d}T, \tag{10}$$

and

$$\mathrm{d}(\Delta g^{\mathrm{trans}}) = -\Delta S^{\mathrm{trans}}\mathrm{d}T - \Delta l^{\mathrm{trans}}\mathrm{d}f, \tag{11}$$

where $\Delta l^{\mathrm{trans}}$ is the actual length change expressed per unit volume. Indeed, $\Delta l^{\mathrm{trans}}$ depends on the shape of the transformed region. This feature will be accommodated in the present formalism by using the resolved stress τ instead of the applied force f [see Eq. (14)].

In Eqs. (9) and (10), the stress dependence of the elastic constants has been neglected, on the basis of the observed linearity in the stress–strain curve up to a 300 MPa stress, which is typical of the Cu-based alloys considered in the present study (see, e.g., [19]).

In Eq. (8) the factor $\partial(I^{\mathrm{inter}})/\partial f$ will be neglected, as a first approximation, in view of the lack of experimental data.

A New τ–T–$\Delta S^{\mathrm{trans}}$ Thermodynamic Relation

By inserting the previous results in Eq. (7), the following condition is obtained:

$$\left[\frac{6r}{c}\frac{\partial(I^{\mathrm{inter}})}{\partial T} + \frac{\pi}{2}\gamma^2 c\frac{(2-\nu)}{(1-\nu)}\frac{\mathrm{d}\mu}{\mathrm{d}T} + \frac{\pi}{2}\gamma^2 c\frac{\mu}{(1-\nu)^2}\frac{\mathrm{d}\nu}{\mathrm{d}T} - 4r\Delta S^{\mathrm{trans}}\right]\mathrm{d}T - 4r\Delta l^{\mathrm{trans}}\mathrm{d}f = 0 \tag{12}$$

which leads to the following relation

$$\frac{\mathrm{d}f}{\mathrm{d}T} = \frac{\left[\frac{3}{2c}\frac{\partial(I^{\mathrm{inter}})}{\partial T} + \frac{\pi}{8}\gamma^2\frac{c}{r}\frac{(2-\nu)}{(1-\nu)}\frac{\mathrm{d}\mu}{\mathrm{d}T} + \frac{\pi}{8}\gamma^2\frac{c}{r}\frac{\mu}{(1-\nu)^2}\frac{\mathrm{d}\nu}{\mathrm{d}T} - \Delta S^{\mathrm{trans}}\right]}{\Delta l^{\mathrm{trans}}}. \tag{13}$$

Starting from this result, a new τ–T–$\Delta S^{\mathrm{trans}}$ relation can be derived by considering that

$$\frac{\mathrm{d}\tau}{\mathrm{d}T} = \frac{s}{A}\frac{\mathrm{d}f}{\mathrm{d}T}, \tag{14}$$

where s is the Schmid factor relating the tensile axis with the crystallographic system for the shear in the habit plane, A is the area of the cross section of the sample, and

$$\Delta l^{\mathrm{trans}} = s\gamma\frac{l}{V} \tag{15}$$

with l being the length of the sample. The Schmid factor allows to connect the strains through $\varepsilon = s\gamma$. By further considering that $V = Al$, Eq. (13) yields

$$\frac{\mathrm{d}\tau}{\mathrm{d}T} = \frac{3}{2}\frac{1}{\gamma}\frac{1}{c}\frac{\partial(I^{\mathrm{inter}})}{\partial T} + \frac{\pi}{8}\gamma\frac{c}{r}\frac{(2-\nu)}{(1-\nu)}\frac{\mathrm{d}\mu}{\mathrm{d}T} + \frac{\pi}{8}\gamma\frac{c}{r}\frac{\mu}{(1-\nu)^2}\frac{\mathrm{d}\nu}{\mathrm{d}T} - \frac{\Delta S^{\mathrm{trans}}}{\gamma}. \tag{16}$$

Equation (16) is the most general result of the current study for a transformation at constant pressure, which reduces to Eq. (1) in two general cases: First, when (r/c) and c increase so that the volume $V[=(r/c)^2c^3]$ approaches the macroscopic limit, as expected. Second, when all dependencies upon temperature are negligible.

Assessment of $\Delta S^{\mathrm{trans}}$ for Cu-Based Shape-Memory Alloys

In the present section, the use of Eq. (16) to refine the evaluation of $\Delta S^{\mathrm{trans}}$ from $\frac{\mathrm{d}\tau}{\mathrm{d}T}$ data in the MT between the close-packed martensites in Cu-based shape-memory alloys will be explored. To this aim, a thermodynamic database including the engineering elastic constants (μ and ν), their temperature dependence, the transformation shear strain, and the interface Gibbs energy is developed in "The Database with Experimental and Estimated Information" section. On these bases, specific forms of Eq. (16), appropriate for Cu–Al–Ni and Cu–Zn–Al alloys are reported in "The Specific τ–T–$\Delta S^{\mathrm{trans}}$ Relation for Cu–Al–Ni and Cu–Zn–Al" section.

The Database with Experimental and Estimated Information

Elastic Constants and Their Temperature Dependencies

The elastic constants C_{ij} of the close-packed 2H structure in Cu–Al–Ni have been measured as a function of temperature by [43]. Similar measurements for the 18R structure in Cu–Zn–Al can be found in [44]. These elastic constants are considered to be representative of those for the compact martensitic phases in each alloy, independent of the structure (2H, 18R, 6R). The elastic constants correspond to the reference system drawn as red squares in Fig. 3. In this plot, the stereographic projection and the Miller indices in black correspond to austenite, and the stereographic triangle indicates the location of the tensile axes which, in traction, can induce the transformation between the latter structures. It is drawn as blue crosses in an arbitrary orthogonal coordinate system with the tensile axis a_{TA} as a first axis.

Starting with the single-crystal elastic constants, an estimation has to be made of the engineering constants ν, μ

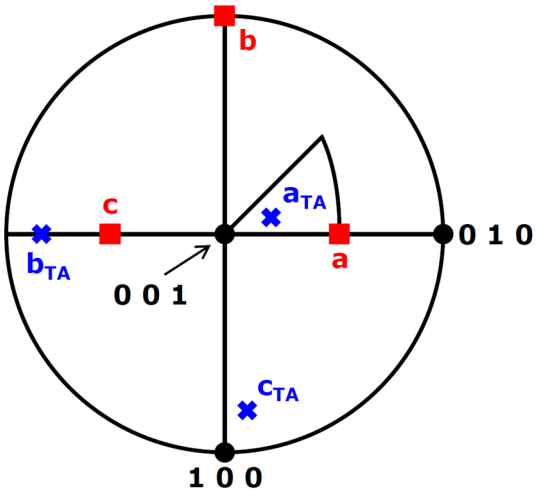

Fig. 3 Stereographic projection along [0 0 1] for the austenite. The main axes (a, b, c) of the stress-induced martensitic variant are shown as red squares. The blue crosses represent an arbitrary coordinate system related to the tensile axis (a_{TA}) located in the usual stereographic triangle. See text for details (Color figure online)

and their temperature dependencies in the martensite. Instead of using the Voigt or Reuss averaging procedures, an attempt was made to specifically account for the nucleation of martensite in the MT between compact structures. This process takes place as a shear deformation in a plane orthogonal to the c axis, in the direction a of the martensite (see red squares in Fig. 3). In this way, the constant μ can be identified with the elastic constant C_{55}. In order to define the Poisson ratio, the guidelines in [45] were accepted by making

$$\nu = -\frac{\varepsilon_O}{\varepsilon_T}, \tag{17}$$

where ε_T is the strain along the tensile direction and ε_O is the strain in an orthogonal direction relative to the tensile axis in the coordinate system drawn as blue crosses in Fig. 3. It should be remarked that although the tensile axis (a_{TA}) is well defined, the choice of the remaining axes b_{TA} and c_{TA} is arbitrary. This coordinate system allows to calculate two values for ν. By rotating around a_{TA}, it is found that the average of the two ν values as well as its temperature dependence are independent of the choice of b_{TA} and c_{TA}, i.e., unique ν and dν/dT values can be determined.

The behavior of ν and dν/dT for the Cu–Al–Ni and Cu–Zn–Al martensites, as calculated from the previous model and referred to the usual stereographic triangle for tensile axes in the austenitic coordinate system, is presented in Fig. 4. In the Cu–Al–Ni system, a maximum of 0.45 for ν occurs in the neighborhood of the $[0\quad 1\quad 2]$ austenite axis and decreases to 0.32 for the $[\bar{1}\ 1\ 1]$ direction (Fig. 4a). In the Cu–Zn–Al martensite, ν shows a maximum of 0.41 for the $[0\quad 0\quad 1]$ austenite axis and decreases to 0.28 when approaching the $[\bar{1}\ 1\ 1]$ direction (Fig. 4b). Furthermore, in Cu–Al–Ni, dν/dT increases when approaching the direction $[0\quad 0\quad 1]$ (Fig. 4c) and the contrary occurs for Cu–Zn–Al (Fig. 4d). In any case, the effect of temperature upon ν is small. In order to estimate the values involved in the Eq. (16), the reported tensile axes (Table 1) were adopted.

The room-temperature elastic constants of the 2H structure for Cu–Al–Ni alloys with two different compositions have also been reported in [46, 47]. The values reported in [46] lead to a dependence of ν upon the choice of the tensile axis similar to that shown before. On the contrary, the elastic constants reported in [47], for an alloy with the lowest Ni content, lead to values of ν behaving similar to Cu–Zn–Al alloys, with a maximum for the tensile axis at $[0\quad 0\quad 1]$. Such discrepancy cannot be explained in terms of the changes in composition or electronic concentration in the material. Nevertheless, the so-obtained values of ν and μ do not differ significantly from those obtained with the first set of elastic constants [43].

Transformation Shear Strain

For the transformation from 18R to 6R, or from 2H to 18R, which occurs on the basal plane, the strain is given by [26]

$$\gamma_{A/B} = \frac{1}{\sqrt{2}}\frac{2\psi^2 - 1}{\psi}(\alpha_A - \alpha_B), \tag{18}$$

where α_I are the corresponding stacking fault densities: $\alpha_{2H} = 0.5$, $\alpha_{6R} = 0$, and $\alpha_{18R} = 0.346$ [48]. The value of ψ is connected to the austenite-to-martensite transformation temperature at zero applied stress (M_S) [49] through

$$\psi = \frac{M_S\ (\mathrm{K}) + 6590}{7320} \tag{19}$$

using the reported M_S values presented in Table 1.

Temperature Dependence of the Interface Gibbs Energy

Direct measurements of the temperature dependence of Γ^{inter} for the systems of interest in the present study were not found in the literature. As a consequence, preliminary estimations were adopted, which were based on measured values of the temperature dependence of the solid/gas surface energy for the elements [50]. Specifically, a weighted average of such quantities, corresponding to the representative compositions Cu–27.3 at.% Al–3.7 at.% Ni and Cu–12.8 at.% Zn–17.6 at.% Al, yielded

$$\frac{\partial(\Gamma^{inter})}{\partial T} = -0.23\,\mathrm{mJ/m^2\,K} = -0.00023\,\mathrm{Pa\,m/K}. \tag{20}$$

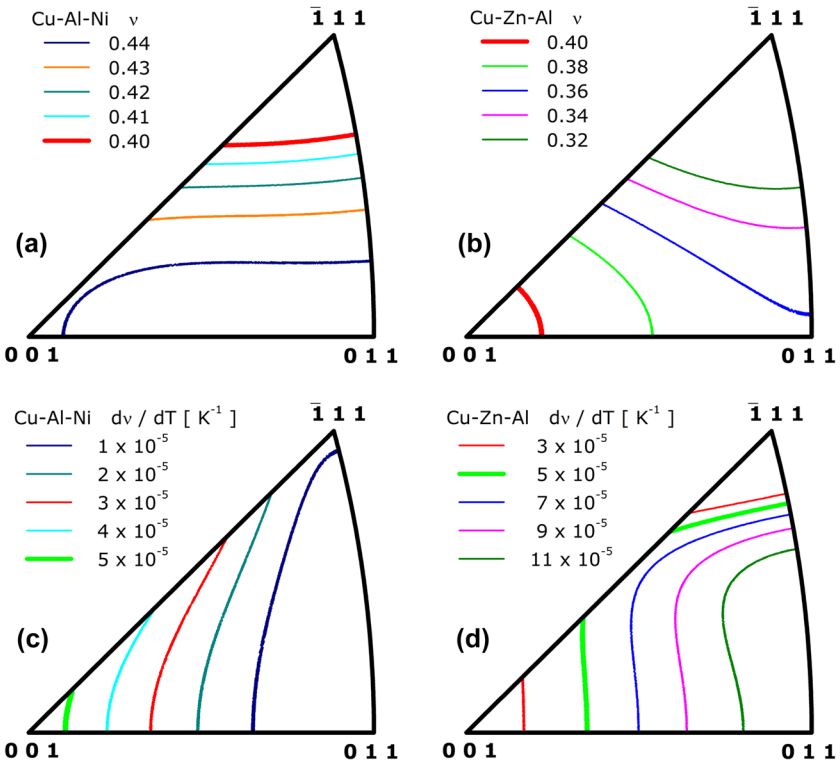

Fig. 4 Calculated mean values of the Poisson ratios ν for **a** Cu–Al–Ni and **b** Cu–Zn–Al martensites presented in the usual austenitic stereographic triangle. In a similar way is presented the temperature dependence of the Poisson ratios for **c** Cu–Al–Ni and **d** Cu–Zn–Al. See text for details

Estimation of the Nucleus Characteristic Parameters

For the evaluation of the semithickness c and the radius r of the nucleus, the values c^* and r^*, respectively, corresponding to a critical embryo, were obtained by applying to Eq. (6) the usual conditions $\left(\frac{\partial \Delta G}{\partial c}\right)_r = 0$ and $\left(\frac{\partial \Delta G}{\partial r}\right)_c = 0$ [51, 52]. This yields

$$c^* = -\frac{2\Gamma^{\text{inter}}}{\Delta g^{\text{trans}}}, \tag{21}$$

$$r^* = \frac{4K^{\text{elast}}\Gamma^{\text{inter}}}{(\Delta g^{\text{trans}})^2}. \tag{22}$$

Due to the lack of direct measurements of Γ^{inter}, estimated values had to be used. The value $\Gamma^{\text{inter}} = 200\,\text{mJ/m}^2$ has been adopted in [37] as typical for solid metallic phases. Similarly, the surface energy correlations given by Chalmers [53] suggest for Cu and some Cu alloys a somewhat larger value, viz., $\Gamma^{\text{inter}} = 250\,\text{mJ/m}^2$. The average $\Gamma^{\text{inter}} = 225\,\text{mJ/m}^2$ was used for the estimate of the nucleus characteristic parameters.

The estimation of Δg^{trans} was based on the results for the Cu–Zn–Al system reported in [26]. Specifically, the enthalpy change was found to present a hysteresis independent of composition and dependent on the transition, implying $\Delta g^{\text{trans}}\,(2\text{H}/18\text{R}) = -2.9\,\text{MJ/m}^3$ and $\Delta g^{\text{trans}}\,(18\text{R}/6\text{R}) = -6.3\,\text{MJ/m}^3$.

Applying a similar procedure to the results for a single Cu–Al–Ni alloy [54] yields $\Delta g^{\text{trans}}\,(2\text{H}/18\text{R}) = -5.6\,\text{MJ/m}^3$ and $\Delta g^{\text{trans}}\,(18\text{R}/6\text{R}) = -11.7\,\text{MJ/m}^3$.

The K^{elast} values defined in Eq. (5) were evaluated using ξ = 0, the elastic constants ("Elastic Constants and Their Temperature Dependencies" section), and the transformation shear strain ("Transformation Shear Strain" section).

The c and r values obtained by inserting the given information in Eqs. (21) and (22) were used to apply Eq. (16) in the following section.

The Specific τ–T–ΔS^{trans} Relation for Cu–Al–Ni and Cu–Zn–Al

By inserting the measured and estimated data discussed above, the values of the first three terms in Eq. (16) (labeled **A**, **B**, and **C**, respectively) and their sum $\boldsymbol{\Omega}$ ($= \mathbf{A} + \mathbf{B} + \mathbf{C}$), such that

$$\frac{\mathrm{d}\tau}{\mathrm{d}T} = \boldsymbol{\Omega} - \frac{\Delta S^{\text{trans}}}{\varepsilon} \tag{23}$$

were evaluated. The results indicate that the least important contribution (labeled **C**) originates in the temperature dependence of ν. As **C** is the only positive term contributing to $\boldsymbol{\Omega}$, the latter adopts negative values.

The $\boldsymbol{\Omega}$ terms calculated for the Cu–Al–Ni and Cu–Zn–Al alloys reported in Table 1 are shown in Fig. 5, distinguishing the data for 2H to 18R from those for 18R to 6R

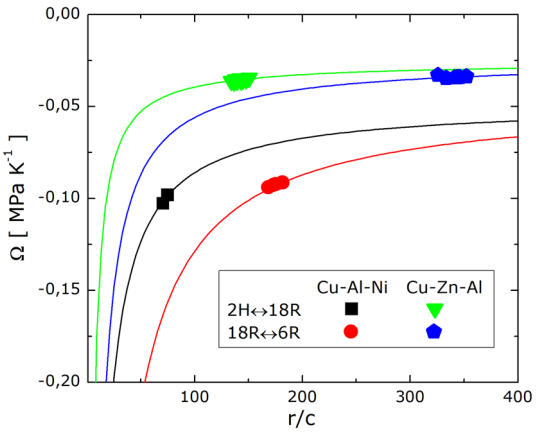

Fig. 5 Calculated **Ω** values as the sum of the three first terms at the right hand side in Eq. (16) for the transitions and alloys presented in Table 1. The lines correspond to the variation of **Ω** as a function of the *r*/*c* variable under constant remaining parameters

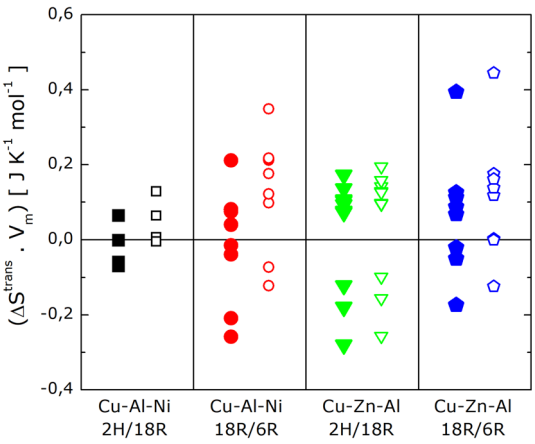

Fig. 6 Entropy differences per unit volume $(\Delta S^{\text{trans}} \cdot V_{\text{m}})$ for the stress-induced transformation between martensitic structures obtained from Eq. (16) (full symbols) and Eq. (1) (open symbols). The specific transition between martensitic phases is indicated at the bottom

transformations. The **Ω** values cluster at specific regions, different for each alloy and transition. The behavior of **Ω** when varying the characteristic parameters of the nucleus is presented as lines in Fig. 5, taking for the remaining parameters their mean values in each of the clustering regions. It can be seen that on increasing the *r*/*c* value, **Ω** decreases asymptotically in magnitude to a constant value. The calculation also shows that for a constant the *r*/*c* ratio, the magnitude of the **Ω** term increases with the decrease of the *c* value.

Another case of interest is that of the squares in Fig. 5, where small variations of the sizes would lead to drastic changes in the **Ω** values. In such conditions, the start of the transition will be highly dependent on the experimental conditions. Hence, a wide range of variation in the measured $\mathrm{d}\tau/\mathrm{d}T$ might be expected.

Assessment of ΔS^{trans}

In this section, Eq. (23) with the **Ω** values in Fig. 5 will be used to evaluate ΔS^{trans} from the available measurements of $\mathrm{d}\tau/\mathrm{d}T$ (Fig. 2). As usual in this field, the entropy differences will be expressed per mol as $\Delta S^{\text{trans}} V_{\text{m}}$, where V_{m} is the molar volume [32]. The resulting entropy differences (full symbols in Fig. 6) are compared with those obtained by the application of Eq. (1) (open symbols in Fig. 6). In both plots a similar scatter can be observed. However, the **Ω** term shifts the experimental cloud to more negative values, making the mean value to fall on $\Delta S^{\text{trans}} \cong 0$. In other words, the comparison made in Fig. 6 suggests that the magnitude of ΔS^{trans} given by Eq. (1) is overestimated.

A similar situation might also occur in the 18R/6R transformations in Cu–Al–Be and Cu–Zn, as for the transitions in Cu–Sn, reported at the end of Table 1. Unfortunately, the lack of experimental data on their elastic properties impeded the proper evaluation of ΔS^{trans} for these alloys.

It should be mentioned, that Wang et al. [55] have modified the CC equation in order to treat various phenomena occurring at the nanoscale in a multifunctional titanium alloy. Beyond the formal similarities with Eq. (16), their approach is conceptually different from the present one, since they intend to represent a stress versus temperature behavior involving three linear ranges. Their phenomenological model does not offer a direct method to estimate entropy differences between the phases involved in MTs.

The present study calls the attention upon the need to take into account the nucleation process when handling the measured $\mathrm{d}\tau/\mathrm{d}T$ values, before making further physical interpretations.

Turning now to the controversy concerning the structure or composition dependence of the average entropy difference between the austenite and martensite, $\Delta S^{\text{mart/aust}}$, the present finding, $\Delta S^{\text{trans}} \cong 0$ for several transformations between martensitic structures and alloy systems, lends support to the early suggestion of $\Delta S^{\text{mart/aust}}$ being independent of the structure of the martensite [26].

Concluding Remarks

Equation (16) expresses the new material-specific relation between ΔS^{trans} and the slope of the experimental τ versus T plots. Instead of the simple proportionality usually adopted following the CC-type relation, the new relation, viz., $\frac{\mathrm{d}\tau}{\mathrm{d}T} = \mathbf{\Omega} - \frac{\Delta S^{\text{trans}}}{\gamma}$, includes a term **(Ω)** involving, among other parameters, the engineering elastic constants and their temperature dependence. Admittedly, the use of

this relation requires additional experimental information, which in many cases is unfortunately not available.

In spite of the approximations necessitated by the lack of direct measurements, the present results indicate that the incorporation of the $\boldsymbol{\Omega}$ term might critically affect the evaluation of ΔS^{trans} for the key MT in Cu-based shape-memory alloys, i.e., the 2H/18R and 18R/6R transformations in Cu–Al–Ni and Cu–Zn–Al shape-memory alloys.

Acknowledgements This study was supported by the ANPCyT, CONICET, CNEA and Universidad Nacional de Cuyo, Argentina.

References

1. Takei F, Miura T, Miyazaki S, Kimura S, Otsuka K, Suzuki Y (1983) Stress induced martensitic transformation in a Ti–Ni single crystal. Scr Metall 17:987–992
2. Romero R, Pelegrina JL (1994) Entropy change between the β phase and the martensite in Cu-based shape-memory alloys. Phys Rev B 50:9046–9052
3. Ahlers M (1986) Martensite and equilibrium phases in Cu–Zn and Cu–Zn–Al alloys. Prog Mater Sci 30:135–186
4. Otsuka K, Wayman CM, Nakai K, Sakamoto H, Shimizu K (1976) Superelasticity effects and stress-induced martensitic transformation in Cu–Al–Ni alloys. Acta Metall 24:207–226
5. Miyazaki S, Otsuka K (1984) Mechanical behaviour associated with the premartensitic rhombohedral-phase transition in a $Ti_{50}Ni_{47}Fe_3$ alloy. Philos Mag A 50:393–408
6. Miyazaki S, Otsuka K (1986) Deformation and transition behavior associated with the R-phase in Ti–Ni alloys. Metall Trans A 17:53–63
7. Stachowiak GB, McCormick PG (1988) Shape memory behaviour associated with the R and martensitic transformations in a NiTi alloy. Acta Metall 36:291–297
8. Pelegrina JL, Ahlers M (1992) The martensitic phases and their stability in Cu–Zn and Cu–Zn–Al alloys—I. The transformation temperature between the high temperature β phase and the 18R martensite. Acta Metall Mater 40:3205–3211
9. Orgéas L, Favier D (1998) Stress-induced martensitic transformation of a NiTi alloy in isothermal shear, tension and compression. Acta Mater 46:5579–5591
10. Šittner P, Novák V, Zárubová N, Studnička V (1999) Stress state effect on martensitic structures in shape memory alloys. Mater Sci Eng A 273–275:370–374
11. Brinson LC, Schmidt I, Lammering R (2004) Stress-induced transformation behavior of a polycrystalline NiTi shape memory alloy: micro and macromechanical investigations via in situ optical microscopy. J Mech Phys Solids 52:1549–1571
12. Otsuka K, Ren X (2005) Physical metallurgy of Ti–Ni-based shape memory alloys. Prog Mater Sci 50:511–678
13. Auguet C, Isalgué A, Lovey FC, Martorell F, Torra V (2007) Metastable effects on martensitic transformation in SMA. Part 4. Thermomechanical properties of CuAlBe and NiTi observations for dampers in family houses. J Therm Anal Calorim 88:537–548
14. Kockar B, Karaman I, Kim JI, Chumlyakov YI, Sharp J, Yu (Mike) C-J (2008) Thermomechanical cyclic response of an ultrafine-grained NiTi shape memory alloy. Acta Mater 56:3630–3646
15. Olbricht J, Yawny A, Pelegrina JL, Dlouhy A, Eggeler G (2011) On the stress-induced formation of R-phase in ultra-fine-grained Ni-rich NiTi shape memory alloys. Metall Mater Trans A 42:2556–2574
16. Delaey L, Chandrasekaran M (1995) Nomenclature of martensites in β-phase alloys. J Phys IV Colloq C2 suppl J Phys III 5(C2):251–256
17. Otsuka K, Sakamoto H, Shimizu K (1975) Martensitic transformations between martensites in a Cu–Al–Ni alloy. Scr Metall 9:491–498
18. Shimizu K, Sakamoto H, Otsuka K (1978) Phase diagram associated with stress-induced martensitic transformations in a Cu–Al–Ni alloy. Scr Metall 12:771–776
19. Otsuka K, Sakamoto H, Shimizu K (1979) Successive stress-induced martensitic transformations and associated transformation pseudoelasticity in Cu–Al–Ni alloys. Acta Metall 27:585–601
20. Sakamoto H, Shimizu K (1987) Pseudoelasticity due to consecutive $\beta_1 \rightleftarrows \beta_1' \rightleftarrows \alpha_1'$ transformations and thermodynamics of the transformation in a Cu–14.4Al–3.6Ni alloy. Trans JIM 28:715–722
21. Sakamoto H, Nakai Y, Shimizu K (1987) Optimization of composition for the appearance of pseudoelasticity due to consecutive $\beta_1 \rightleftarrows \beta_1' \rightleftarrows \alpha_1'$ transformations in Cu–Al–Ni alloy single crystals. Trans JIM 28:765–772
22. Barceló G, Ahlers M, Rapacioli R (1979) The stress induced phase transformation in martensitic single crystal of CuZnAl alloys. Z Metallkde 70:732–738
23. Saburi T, Inada Y, Nenno S, Hori N (1982) Stress-induced martensitic transformations in Cu–Zn–Al and Cu–Zn–Ga alloys. J Phys 43(C4):633–638
24. Sato H, Takezawa K, Sato S (1984) Analysis of stress–strain curves in the tensile test of Cu–Zn–Al alloy single crystals. Trans JIM 25:332–338
25. Pelegrina JL (1990) Estabilidad de fases martensíticas en aleaciones de Cu–Zn–Al (Stability of martensitic phases in Cu–Zn–Al alloys). Doctoral Thesis, Instituto Balseiro, Universidad Nacional de Cuyo, Argentina (in Spanish)
26. Ahlers M, Pelegrina JL (1992) The martensitic phases and their stability in Cu–Zn and Cu–Zn–Al alloys—II. The transformation between the close packed martensitic phases. Acta Metall Mater 40:3213–3220
27. Arneodo Larochette P, Condó AM, Ahlers M (2005) Stability and stabilization of 2H martensite in Cu–Zn–Al single crystals. Philos Mag 85:2491–2525
28. Hautcoeur A, Eberhardt A, Patoor E, Berveiller M (1995) Thermomechanical behaviour of monocrystalline Cu–Al–Be shape memory alloys and determination of the metastable phase diagram. J Phys IV 5(C2):459–464
29. de Castro Bubani F, Sade M, Torra V, Lovey F, Yawny A (2013) Stress induced martensitic transformations and phases stability in Cu–Al–Be shape-memory single crystals. Mater Sci Eng A 583:129–139
30. Kato H, Miura S (1995) Thermodynamical analysis of the stress-induced martensitic transformation in Cu–15.0 at.% Sn alloy single crystals. Acta metall mater 43:351–360
31. Schroeder TA, Wayman CM (1978) Martensite-to-martensite transformations in Cu–Zn alloys. Acta Metall 26:1745–1757
32. Romero R, Pelegrina JL (2003) Change of entropy in the martensitic transformation and its dependence in Cu-based shape memory alloys. Mater Sci Eng A 354:243–250
33. Obradó E, Mañosa L, Planes A (1997) Stability of the bcc phase of Cu–Al–Mn shape-memory alloys. Phys Rev B 56:20–23
34. Olson GB, Cohen M (1975) Thermoelastic behavior in martensitic transformations. Scr Metall 9:1247–1254
35. Laplanche G, Birk T, Schneider S, Frenzel J, Eggeler G (2017) Effect of temperature and texture on the reorientation of martensite variants in NiTi shape memory alloys. Acta Mater 127:143–152

36. Olson GB, Roitburd AL (1992) Martensitic nucleation. In: Olson GB, Owen WS (eds) Martensite. A tribute to Morris Cohen. ASM International, Materials Park, pp 149–174
37. Kaufman L, Cohen M (1958) Thermodynamics and kinetics of martensitic transformations. Prog Met Phys 7:165–246
38. Kaufman L, Hillert M (1992) Thermodynamics of martensitic transformations. In: Olson GB, Owen WS (eds) Martensite. A tribute to Morris Cohen. ASM International, Materials Park, pp 41–58
39. Olson GB, Cohen M (1986) Dislocation theory of martensitic transformations. In: Nabarro FRN (ed) Dislocations in solids, vol 7. Elsevier Science Publishers, Amsterdam, p 297
40. Olson GB, Cohen M (1976) A general mechanism of martensitic nucleation: Part I. General concepts and the FCC → HCP transformation. Metall Trans A 7:1897–1904
41. Eshelby JD (1957) The determination of the elastic field of an ellipsoidal inclusion, and related problems. Proc R Soc Lond A 241:376
42. Chen Y, Schuh CA (2011) Size effects in shape memory alloy microwires. Acta Mater 59:537–553
43. Landa M, Sedlák P, Šittner P, Seiner H, Heller L (2008) On the evaluation of temperature dependence of elastic constants of martensitic phases in shape memory alloys from resonant ultrasound spectroscopy studies. Mater Sci Eng A 481–482:567–573
44. Gonzàlez-Comas A, Mañosa L, Planes A, Lovey FC, Pelegrina JL, Guénin G (1997) Temperature dependence of the second-order elastic constants of Cu–Zn–Al shape-memory alloy in its martensitic and β phases. Phys Rev B 56:5200–5206
45. Rovati M (2003) On the negative Poisson's ratio of an orthorhombic alloy. Scr Mater 48:235–240
46. Sedlák P, Seiner H, Landa M, Novák V, Šittner P, Mañosa L (2005) Elastic constants of bcc austenite and 2H orthorhombic martensite in CuAlNi shape memory alloy. Acta Mater 53:3643–3661
47. Yasunaga M, Funatsu Y, Kojima S, Otsuka K (1983) Measurement of elastic constants. Scr Metall 17:1091–1094
48. Lovey FC (1987) The fault density in 9R type martensites: a comparison between experimental and calculated results. Acta Metall 35:1103–1108
49. Ahlers M (1974) On the stability of the martensite in β-Cu–Zn alloys. Scr Metall 8:213–216
50. Aqra F, Ayyad A (2011) Surface energies of metals in both liquid and solid states. Appl Surf Sci 257:6372–6379
51. Raghavan V, Cohen M (1972) A nucleation model for martensitic transformations in iron-base alloys. Acta Metall 20:333–338
52. Raghavan V, Cohen M (1972) Growth path of a martensitic particle. Acta Metall 20:779–786
53. Chalmers B (1962) Physical metallurgy. Wiley, New York
54. Otsuka K, Sakamoto H, Shimizu K (1976) Two stage superelasticity associated with successive martensite-to-martensite transformations. Scr Metall 10:983–988
55. Wang HL, Hao YL, He SY, Li T, Cairney JM, Wang YD, Wang Y, Obbard EG, Prima F, Du K, Li SJ, Yang R (2017) Elastically confined martensitic transformation at the nano-scale in a multifunctional titanium alloy. Acta Mater 135:330–339